S = area, cm^2
T = temperature, K or °C
u = molar average velocity, cm/s
U = heat transfer coefficient, kcal/cm^2 · s · K
V = reactor volume, liter
W = rate of internal heat generation, kcal/liter-hr
W_c, W_I = spectrographic slit width, cm
x = length along arc, cm
X = conversion, fraction
X_0 = exit conversion, percent or fraction
X' = conversion variable (defined by Equation (15), Part II), percent or fraction
Y = mole fraction
z = length along reactor, cm

Greek Letters

α = defined by Equation (11), Part II
β = defined by Equation (12), Part II
ϵ = molecular extinction coefficient, liter/gmol-cm
λ = wavelength, Å
ν = wave number, cm^{-1}
ϕ = angle, radians
Φ = quantum yield, gmol/einstein
ψ = light absorption function (defined by Equation (16), Part I)
θ = angle, radians

Subscripts

1 = outer radius
c = during calibration
eff = effective
i, j = species i or j
normal distance across reaction annulus
l = limiting reactant
m = mean value
0 = inlet to reactor
lower limiting value
inner radius
r = radial direction
s = surroundings
z = axial direction

LITERATURE CITED

Bonhoeffer, K. F., "Application of Quantum Theory to Photochemical Sensitizing," *Z. Phys.*, **13**, 94 (1923).

Calvert, J. G. and J. N. Pitts, *Photochemistry*, Wiley, New York (1966).

LeBlanc, M., K. Andrich, and W. Kangro, "Photochemische Umsetzungen im System $SO_2CL_2 \rightleftarrows SO_2 + Cl_2$ unter dem Einfluss von Strahlen Bestimmter Wellenlänge," *Z. Elektroch.*, **25**, 229 (1919).

Londergan, M. C., "The Photochemistry of the Formation of Sulfuryl Chloride," *Iowa State Coll. J. Sci.*, **17**, 95 (1942-43).

Noyes, R. M., "Wall Effects in Photochemically Induced Chain Reactions," *J. Am. Chem. Soc.*, **73**, 3039 (1951).

Schumacher, H. J., and C. Schott, "Die Photochemische Bildung von Sulfurylchlorid in der Gasphase aus Schwefeldioxyd und Chlor und sein durch Chlor Sensibilisierter Zerfall," *Z. Phys. Chem.*, **193**, 343 (1942-43).

Szabo, A. G., and T. Berces, "Der Mechanismus des Thermischen Zerfalls von Sulfurylchlorid," *Z. Phys. Chem.*, **12**, 168 (1957).

———., and P. Huhn, "Vollstandige Kinetische Analyse des Mechanismus des Thermischen Sulfurylchloridzerfalls," *ibid.*, **23**, 70 (1960).

Trautz, M., "Thermodynamics of Sulfuryl Chloride Equilibrium. IV. Velocity of the Reaction Approaching Equilibrium," *Z. Elektroch.*, **21**, 329 (1915).

Manuscript received July 16, 1973; revision received August 31 and accepted September 4, 1973.

Developing Pressure Profiles for Non-Newtonian Flow in an Annular Duct

A steady, laminar, isothermal flow of non-Newtonian fluids in the entrance region of an annulus has been studied experimentally. The axial pressure distributions, as well as the excess pressure energy, in the developing flow region are presented. The loss coefficients are found to increase with increasing flow behavior index for inelastic power law fluids. The experimental values of the loss coefficients are about 20% lower than those predicted from the boundary-layer approximation method presented earlier. A preliminary result indicates that the entrance loss for a viscoelastic fluid is much smaller than that for the inelastic fluid of the same flow behavior index.

SATINATH BHATTACHARYYA and CARLOS TIU

Department of Chemical Engineering
Monash University
Clayton, Victoria 3168, Australia

SCOPE

The problem of the developing flow of non-Newtonian fluids in the entrance region of an annulus is important because of its application in many polymer processing industries and in heat exchangers. Very little information concerning this area of research is available in the literature. When a fluid enters an annulus through a flow straightener followed by an abrupt contraction, it undergoes a change in the flow pattern from a reasonably flat velocity profile at the entrance to a fully-developed profile at a certain distance downstream. The change in the velocity causes an increase in the fluid kinetic energy and an increase in viscous friction associated with a loss in pressure energy which is larger than that experienced in the fully developed region. The object of the present study is to determine experimentally the axial pressure distribution for the developing flow of non-Newtonian fluids in the entrance region of an annular duct, thus providing a measure of the excess pressure losses in the entrance region. The experimental results will also serve to justify the theoretical analyses presented by the authors (1973) in an earlier paper.

CONCLUSIONS AND SIGNIFICANCE

The significance of the present study lies in the accurate estimation of the excess energy losses for laminar non-Newtonian flow in the entrance region of an annulus. The entrance losses, as expressed in terms of loss coefficient, are found to increase with increasing flow behavior index for inelastic power-law fluids. The experimental results are also used to justify theoretical predictions presented by the authors (1973). The results indicate that theoretically predicted loss coefficients are about 20% higher than those obtained experimentally. The discrepancy is due to a smaller pressure drop being observed between the first two pressure taps immediately after the contraction. The low pressure drop is a result of a skewed velicity profile at the entry. A perfectly flat entry profile, as is assumed in the theoretical analysis, is exceedingly difficult to simulate in the laboratory. A flow straightener inserted in the upstream side of the contraction is needed not only for generating a reasonably flat entry velocity profile but also to reduce the effects of vena contracta at the downstream side over the experimental Reynolds number range. Results obtained for a higher concentration polymer solution indicate that the entrance losses for a viscoelastic fluid are much smaller than those obtained for the inelastic fluid of the same flow behavior index. The hydrodynamic entrance length, defined as the distance from the entry to the position where the maximum velocity reaches 98% of its fully developed value, cannot be accurately established from the pressure measurements but must be obtained from velocity profile measurements.

The study of the developing flow in the entrance region of a concentric annulus is of significance because of many important engineering applications such as in heat exchangers, axial flow turbo-machinery, and in polymer processing industries. For a fluid entering an annulus in laminar flow through an abrupt contraction a development of the velocity profile takes place from an initial condition close to a flat velocity profile at the inlet to a fully developed condition at a certain distance downstream. The distance from the contraction to the point where the maximum velocity is 98% of its fully developed value is presently defined as the hydrodynamic entrance length. For inelastic liquids the pressure drop per unit length in this section is higher than that in the fully developed region. This entrance section, although not very long, may contribute a significant influence to the overall pressure drop and must be taken into account in design.

In spite of the importance of this developing flow, relatively little experimental or theoretical research has been carried out. A number of papers (Rothfus, 1955; Olson and Sparrow, 1963; Sparrow and Lin, 1964; Lundgren, Sparrow and Starr, 1964; Okiishi and Serovy, 1967; and Wilson and Medwell, 1971) concerned with the flow of Newtonian fluids in the entrance region of annuli have appeared in the literature. Recently, the authors (1973) presented theoretical analyses based on boundary layer approximations and on linearization techniques to describe the flow behavior of power-law fluids in the entrance region of annuli.

All the experimental works reported in the literature on Newtonian fluids have been carried out in the turbulent flow region. The results presented by Rothfus (1955), Olson and Sparrow (1963), Okiishi and Serovy (1967), and Wilson and Medwell (1971) showed considerable differences in the magnitude of the entrance pressure losses and the entry length. The deviation could be attributed to the differences in the entry geometries used by these investigators. In the experimental work relating to the annular entry flow three different geometries of the entry are normally used, namely, square entrance, rounded entrance, and a square entrance with the inner tube extending to the upstream side of the contraction. The latter geometry, which is an intermediary between the square and the rounded entrance, is used in the present investigation. Okiishi and Serovy experimentally observed the development of the hydrodynamic boundary layer for annular turbulent flow using both square-edged and rounded entrances. They found that the entrance length for the square-edged geometry was much shorter than for the rounded one. The difference was attributed to the fact that for the latter geometry there is a transition from the laminar boundary layer to the turbulent boundary layer in the entrance region, in contrast to the former case where no such transition existed.

In the study of non-Newtonian flow in annuli, the excess pressure drop in the entrance region may become significant even under laminar flow conditions. The present study is concerned with the experimental measurement of axial pressure distributions and the excess pressure losses for laminar flow of non-Newtonian fluids in the entrance region of an annular duct. All the liquids used in the present study behaved as inelastic non-Newtonian fluids except one which showed viscoelastic behavior.

It can be shown by applying a mechanical energy balance on a fluid between the inlet section of an annulus where the velocity profile is assumed uniform and a section at a distance sufficiently downstream for the velocity profile to be fully developed (see Figure 1) that

$$(P_1 - P_2)/\tfrac{1}{2}\rho\langle u\rangle^2 = 16x/r_H Re + C \qquad (1)$$

where $(P_1 - P_2)$ is the pressure drop from just inside the inlet section to any distance x beyond the entrance region, and the correction factor C is the loss coefficient.

For a power-law fluid in which the non-Newtonian viscosity is defined by

$$\frac{1}{\eta} = (1/\tau)(\tau/K)^{1/n} \qquad (2)$$

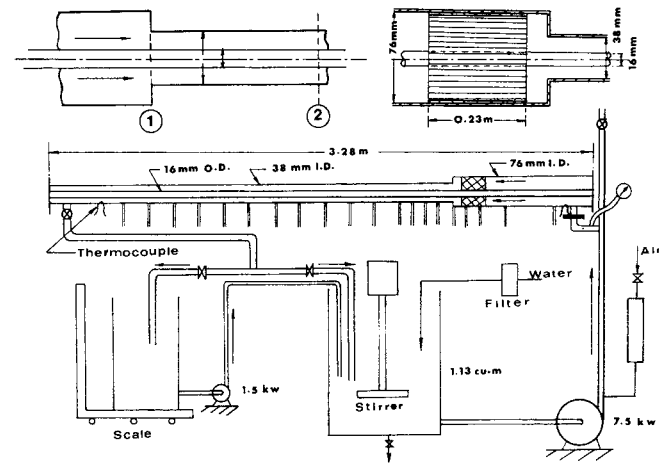

Fig. 1. Schematic diagram of the annular flow system.

the Reynolds number for laminar annular flow is defined by Kozicki et al. (1966, 1971) as follows:

$$Re = \frac{16}{f} = \frac{2^{3-n} r_H{}^n \langle u \rangle^{2-n} \rho}{K \left[\frac{\epsilon_0 n + \epsilon_1}{n} \right]^n} \qquad (3)$$

where the hydraulic radius $r_H = D_o(1-k)/4$, and ϵ_0 and ϵ_1 are the two primary geometric parameters characterizing the flow geometry. Values of ϵ_0 and ϵ_1 are tabulated as functions of the aspect ratio $k = D_i/D_o$ in the papers of Kozicki et al. The above Reynolds number reduces to the conventional circular pipe Reynolds number for power-law fluids with $\epsilon_0 = 0.75$ and $\epsilon_1 = 0.25$.

The loss coefficient C can be readily obtained from the experimentally measured axial pressure distribution and volumetric flow rate using Equation (1). The experimental results are used to substantiate the theoretical predictions based on the boundary layer approach presented earlier (1973).

EXPERIMENTAL APPARATUS AND PROCEDURES

A schematic diagram of the flow system is presented in Figure 1. The liquid was pumped from a 1.13-m³ (200-gallon) tank by means of a 7.5-kw monopump fitted with a surge tank in the delivery line. The liquid flowed through the annular space between a 76-mm I.D. copper pipe and a 16-mm O.D. stainless steel pipe before entering the annular test section. The concentric annular test section consisted of a smooth outside copper pipe of 38 mm I.D. and an inner pipe extended from the upstream side of the contraction, as shown in Figure 1. This provided an aspect ratio k of 0.417 for the annular test section. The liquid flowed back to the 1.13 m³ tank by means of an overhead line. Pressure actuating valves were installed to divert the flow to a 0.25-m³ (44-gal) tank mounted on a 250-kg platform scale for the purpose of flow rate measurements. A 1.5 kw monopump was used to pump the liquid back from the 0.25-m³ tank to the 1.13-m³ tank.

Pressure tappings were carefully mounted on the outer pipe of the annular test section with the first tap being installed right at the contraction. The distance between two pressure taps for the first five taps was 76 mm while the rest of the pressure taps were placed at 152.5 mm intervals. Seventeen pressure taps were connected to a manometer manifold. Meriam oil of specific gravity 1.75 was used as manometer fluid. Copper-Constantan thermocouples were fixed at the inlet and outlet positions of the test section to measure the temperature of the flowing liquid and to ensure that viscous heating effects were not significant.

In order to generate an approximately flat velocity profile at the inlet of the test section, a 0.23-m flow straightener consisting of a bundle of 6.5-mm stainless steel tubes (also shown in Figure 1) was installed in the upstream section of the annulus at a distance of 38 mm from the contraction.

Before collecting any test data, the apparatus was run for about an hour so that steady state could be reached. Once the steady state was attained the pressure drops across all the taps, the liquid inlet and outlet temperatures, and the mass flow rate were recorded. Mass flow rates were measured by noting the time required to collect 50 kg. of the liquid in the 0.25-m³ tank.

Liquid samples were collected before and after each test run and were analyzed using an R-16 Weissenberg Rheogoniometer equipped with a cone-and-plate combination of diameter 75 mm and cone angle 1°23′. Shear stress and first normal stress difference were measured as a function of shear rate. Evaporation effects were eliminated by applying a coating of silicone oil at the edge of the cone-and-plate assembly after the sample was loaded. The temperature of the liquid sample was controlled to within ± 0.5°C. The test fluids used in this work were aqueous solutions of cellulose gum, Methocel, and Carbopol. During the course of an experiment on the flow system, no shear degradation was observed for all the solutions, though Carbopol solutions showed signs of degradation with time and with the continuous application of shear stress over a long period of time.

RESULTS AND DISCUSSION

The relevant rheological properties of the power-law fluids used in the experiment on the flow system are tabulated in Table 1. All the test solutions exhibited inelastic behavior except for the 2% cellulose gum which exhibited a measurable first normal stress difference at the wall shear rate employed in the flow system.

The experimental pressure drops and flow rates for fully-developed annular flow are presented as the friction factor-Reynolds number chart in Figure 2, where Re is defined by Equation (3). The main advantage of adopting the present definition of Reynolds number is that all fully-developed laminar flow data can be correlated by the familiar pipe flow relationship $f = 16/Re$ regardless of the flow geometry. This relationship is represented by the solid line shown in Figure 2. The average deviation between the theoretical and experimental results is about ± 5%. This not only serves to justify the accuracy of the technique, but also lends additional support to the

TABLE 1.* RHEOLOGICAL PROPERTIES OF POWER-LAW FLUIDS INVESTIGATED AND LOSS COEFFICIENTS

Fluid	Concentration, wt. %	n	K ($N\,s^n\,m^{-2}$)	C_{Exp}	C_{Theo}
Methocel	0.30	0.86	0.044	0.49	0.60
	0.34	0.82	0.062	0.46	0.59
	0.40	0.79	0.090	0.44	0.57
	0.49	0.75	0.060	0.43	0.55
	0.53	0.68	0.325	0.42	0.53
Cellulose gum	0.67	0.91	0.039	0.52	0.62
	0.91	0.88	0.057	0.49	0.61
	1.20	0.84	0.096	0.45	0.59
	2.00**	0.76	0.580	0.10	0.56
Carbopol	0.08	0.66	0.110	0.38	0.52

* All the rheological properties were measured at 20° ± 0.5°C and over a shear rate range of 30 to 1,300 s^{-1}.

** 2% cellulose gum exhibited measurable first normal stress difference from 19.8 to 152.0 N/m^2 in the above shear rate range.

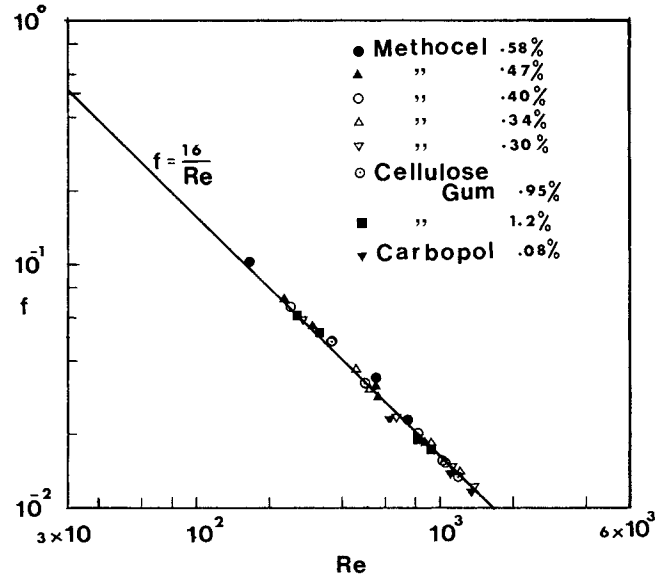

Fig. 2. Friction factor-Reynolds number plot.

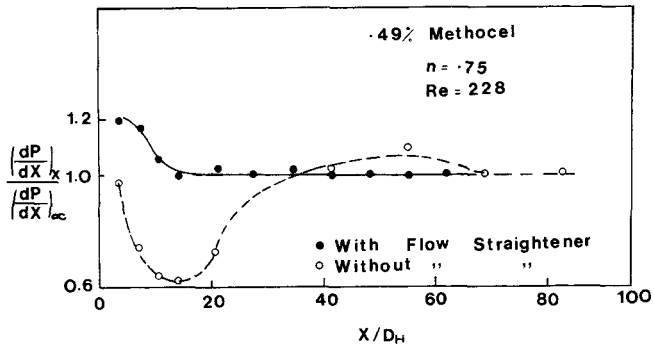

Fig. 3. Dimensionless pressure gradient as a function of axial distance.

geometric parameter method proposed by Kozicki et al. (1966, 1971). An independent check which yielded the same degree of accuracy was also made by comparing the experimental results with the theoretical solution of Fredrickson and Bird (1958) for power-law flow in annuli.

In order to illustrate the nature of the axial pressure distribution in the entrance region of an annulus, the experimental results obtained for the 0.49% Methocel solution at $Re = 228$ are plotted in the form of dimensionless pressure gradient versus axial distance, as shown in Figure 3. The solid and dotted curves represent the best fitted curves passing through the experimental points obtained with and without the flow straightener, respectively. The general trend of the pressure gradient curves agree with those obtained by Olson and Sparrow (1963) for the turbulent flow of Newtonian fluids in annuli. The dotted curve shows that a minimum point in the pressure gradient exists at about $x/D_H = 15$ and that the gradient gradually increases to a maximum at about $x/D_H = 55$ before it levels off to the fully-developed value. This could be attributed to the presence of a vena contracta at the minimum position due to sudden contraction followed by the expansion of fluid cross section until the main fluid stream occupies the entire annular section at about the maximum location. However, with the flow straightener in the upstream side, the fluid enters the contraction more uniformly—the pressure gradient is maximum at the contraction and gradually decreases until it becomes uniform somewhere in the downstream section. All the experimental results presented in this paper have been obtained with the flow straightener. It should be also pointed out that in any of the experimental runs when $Re > 800$, the pressure drop between the first two taps immediately after the contraction was found to be less than the corresponding drop between the subsequent taps, which indicated that as the flow rate was increased the vena contracta became more predominant. For this reason the upper limit of Reynolds number employed in the experiments was kept at about 1300 because any flow rate above this Reynolds number produced a very significant drop in pressure in the first axial position. It can be seen from Figure 3 that even at a much lower Reynolds number, in this case $Re = 228$, the pressure drop measured between the first two taps, represented by the first solid point, is much smaller than the value which would be expected if the smooth curve drawn through the axial pressure gradients measured at subsequent axial positions were extrapolated back to the initial position. This low pressure gradient is a result of a skewed velocity profile at the entry. A perfectly flat entry profile, as is assumed in the theoretical analysis, is extremely difficult to achieve experimentally even in the presence of a flow straightener upstream.

It must be pointed out that although a qualitative estimate of the entrance length can be taken as the distance from the contraction to the point where the pressure gradient becomes constant, an accurate entrance length cannot be established because of the insensitivity of pressure drop over a small length of the annular section. A more accurate method of establishing annular entrance length is from the velocity profile measurements. This project is currently under investigation.

Figure 4 is a typical plot of dimensionless pressure drop $\Delta P/\frac{1}{2}\rho\langle u\rangle^2$ versus dimensionless axial distance $x/r_H Re$ obtained for the 0.34% Methocel solution. The Reynolds numbers covered in the experiment range from $515 \leq Re \leq 1190$. It is evident that the pressure gradient in the entrance region is not constant, but higher than that in the fully developed region. Beyond the entrance region, the experimental data can be represented by a straight line with a slope of 16, which is consistent with Equation (1). The experimental results obtained for all the test liquids have been plotted in a similar fashion. The plots were subsequently used to determine the loss coefficients. Experimental values of C are tabulated in Table 1 together with the theoretical predictions obtained in the boundary-layer approximation (momentum-energy integral method). These values are also plotted in Figure 5 as functions of flow behavior index, with the solid curve representing the theoretical predictions. The experimental loss coefficients are seen to increase with increasing n, which is in agreement with the predicted trend for inelastic fluids. The predicted values of C are more conservative and are about 20% larger than the experimental values over a wide range of flow behavior index. As pointed out earlier, the measured pressure drop in the first axial position is always smaller than the expected

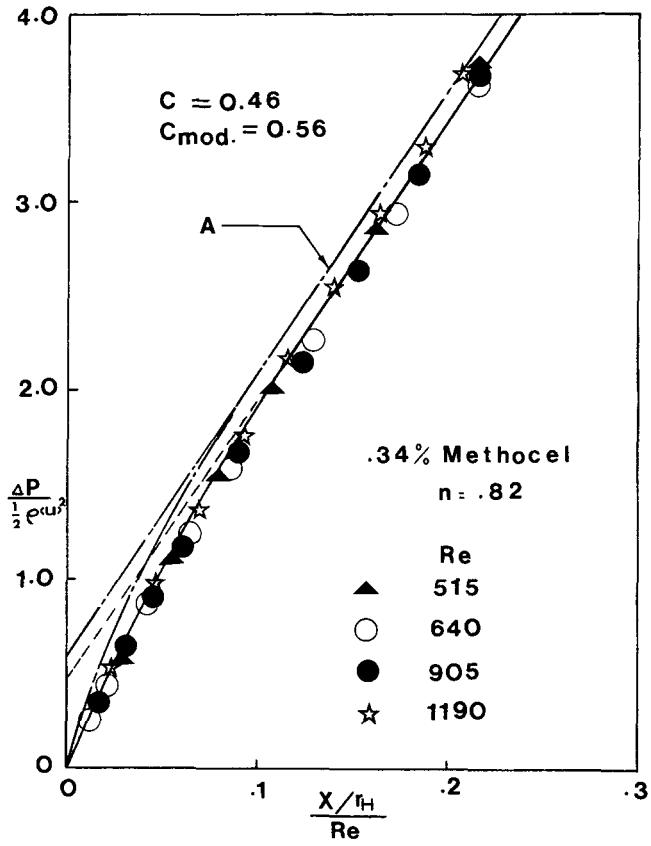

Fig. 4. Dimensionless pressure drop as a function of axial distance.

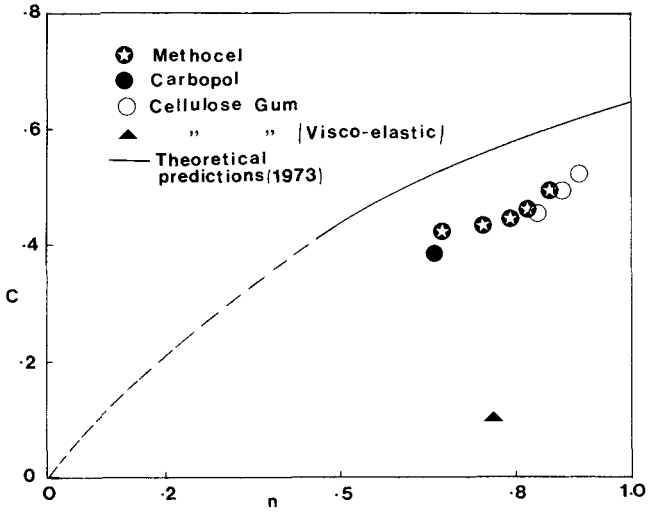

Fig. 5. Loss coefficient as a function of flow behavior index.

value. Since the experimental loss coefficient was obtained from the cumulative axial pressure drop over the entire distance of the annulus, a discrepancy in the first axial pressure measurement could easily shift the axial pressure drop to yield a different value of the intercept on the pressure drop-distance plot as shown in Figure 4. In order to justify the argument just presented, an attempt was made to modify the loss coefficients by determining the pressure gradient at the first axial position from an extrapolation of pressure gradients measured at subsequent axial positions. This modification resulted in a constant factor shift in the $\Delta P/\frac{1}{2}\rho<u>^2$ versus $x/r_H Re$ curve, which yielded a different value of the loss coefficient. The modified curve for the 0.34% Methocel solution is represented by curve A in Figure 4 which shows a modified loss coefficient of 0.56 as compared to the original value of 0.46. The theoretical loss coefficient predicted from the boundary layer theory for this particular fluid is 0.586.

Work is being extended to investigate the influence of elasticity on the annular entrance losses. A preliminary result is presented to indicate the difference in flow behavior of an inelastic fluid and a viscoelastic fluid in the developing flow region. Although most polymer solutions would be expected to show some viscoelastic characteristics under certain flow conditions, the fluids were considered to be viscoelastic when there was a measurable normal stress in the experimental shear rate range. In the present study all the test fluids were inelastic except for the 2% cellulose gum solution which exhibited a measurable first normal stress difference ranges from 19.8 to 152 N/m^2 over a shear rate range of 30 to 1300 s^{-1}. The loss coefficient obtained for the 2% cellulose gum solution is 0.1 as compared to 0.43 for the inelastic fluid at the same flow behavior index. This finding is consistent with that observed by Boger and Rama Murthy (1970) for the viscoelastic flow in the entrance region of circular pipes. They observed experimentally that the velocity profiles for certain viscoelastic fluids were already fully developed at the contraction, resulting in no entrance loss. However, their results appeared to hold only over a limited range of wall recoverable shear. The same argument could be applied in the present case. The velocity profile at the annular contraction for a viscoelastic fluid could be partially, if not fully, developed, resulting in lower losses. Additional experimental evidence must be obtained, particularly the velocity profile measurements, to ascertain this observation.

ACKNOWLEDGMENT

The authors wish to acknowledge the financial support of the Australia Research Grant Committee.

NOTATION

C = loss coefficient defined by Equation (1)
D_H = $D_o - D_i$, hydraulic diameter, D_o and D_i refer to the outer and inner pipe diameters of the annular test section
f = Fanning friction factor
k = D_i/D_o, aspect ratio
K = fluid consistency index for power-law fluid
P_1 = pressure at the inlet
P_2 = pressure at any distance x from the inlet
dP/dx = pressure gradient at any axial position; subscript ∞ refers to the fully-developed region
r_H = $D_H/4$, hydraulic radius
Re = Reynolds number defined by Equation (3)
$<u>$ = average velocity
u_{max} = maximum velocity
x = axial distance from the inlet

Greek Letters

ϵ_0, ϵ_1 = primary geometric parameters defined by Kozicki and Tiu (1971); $\epsilon_0 = 1.000$ and $\epsilon_1 = 0.481$ for the annular test section
ρ = liquid density
η = non-Newtonian viscosity
τ = shear stress

LITERATURE CITED

Boger, D. V., and A. V. Ramamurthy, "Experimental measurements of loss co-efficients in the entrance region of a pipe for viscous power law and viscoelastic fluids," *AIChE J.*, **16**, 6, 1088 (1970).

Bogue, D. C., "Entrance effects and prediction of turbulence in non-Newtonian flow," *Ind. Eng. Chem.*, **51**, 874 (1959).

Fredrickson, A. G., and R. B. Bird, "Non-Newtonian flow in annuli," *ibid.*, **50**, 348 (1958).

Kozicki, W., C. H. Chou, and C. Tiu, "Non-Newtonian flow in ducts of arbitrary cross sectional shape," *Chem. Eng. Sci.*, **21**, 665 (1966).

Kozicki, W., and C. Tiu, "Improved parametric characterization of flow geometries," *Can. J. Chem. Eng.*, **49**, 562 (1971).

Lundgren, T. S., E. M. Sparrow, and J. B. Starr, "Pressure drop due to the entrance region in ducts of arbitrary cross section," *J. Basic Eng., Trans. ASME*, **86D**, 620 (1964).

Okiishi, T. H., and G. K. Serovy, "An experimental study of the turbulent flow boundary layer development in smooth annuli," *ibid.*, **89D**, 823 (1967).

Olson, R. M., and E. M. Sparrow, "Measurements of turbulent flow development in tubes and annuli with square or rounded entrances," *AIChE J.*, **9**, 766 (1963).

Rothfus, R. R., K. G. Monrad, K. G. Sikchi, and W. J. Heideger, "Isothermal skin friction in flow through annular sections," *Ind. Eng. Chem.*, **47**, 5, 913 (1955).

Sparrow, E. M., and S. H. Lin, "The developing laminar flow and pressure drop in the entrance region of annular ducts," *J. Basic Eng., Trans. ASME*, **86D**, 827 (1964).

Tiu, C., and S. Bhattacharyya, "Flow behaviour of power law fluids in the entrance region of annuli," *Can. J. Chem. Eng.*, **51**, 47 (1973).

Wilson, N. W., and J. O. Medwell, "An analysis of the developing turbulent hydrodynamic and thermal boundary layers in an internally heated annulus," *J. Heat Transfer*, Trans. ASME, **93C**, 25 (1971).

Manuscript received May 16, 1973; revision received September 25 and accepted September 26, 1973.